

Oval-Parabola Trajectories (OPT) Model of Droplet-Wall Interaction in Engine

K.Naitoh and Y.Takagi

*NISSAN Motor Co., Ltd.
1 Natsushima-cho, Yokosuka-shi 237
Japan*

ABSTRACT

A theoretical model based on a nonlinear ordinary differential equation was developed, which can estimate the breakup process of droplets after wall impingement. The model is called the Oval-Parabola Trajectories (OPT) model from the trajectory characteristics.

Comparisons made with some fundamental experimental data confirm that this mathematical model is effective in a wide range of Weber number.

A previously reported numerical code based on the multi-level formulation and the renormalization group theory are combined with the OPT model. Secondary atomization behavior on valve surfaces in spark-ignition engine is analysed by using the model.

INTRODUCTION

Mathematical models of the breakup process caused by air-droplet, droplet-droplet, and droplet-wall interactions are required to perform the numerical predictions of the liquid fuel distribution in gasoline engines;

Recent studies for the air-droplet interaction have produced some effective mathematical models based on linear analysis [1][2].

The development of the theoretical model for the breakup process of droplet after wall impingement becomes a bottleneck for realizing an entire model of engine performance predictions.

In the present research, a theoretical model for the droplet-wall interaction was developed by

deriving a nonlinear ordinary differential equation governing the distortion and oscillation of droplets. The trajectory of this equation varies from an oval to a parabola in the phase space of droplet distortion and its speed, due to the increase in the initial velocity and distortion. Four regimes for the diameter distribution of child droplets can be predicted from the complex feature of the equation. The amount of liquid film remaining on the wall and the number of the broken droplets are estimated by the mass and energy conservation laws. The resulting theoretical model is called the Oval-Parabola Trajectories (OPT) model from the trajectory characteristics.

Comparisons with some fundamental experimental data indicate that this mathematical model can predict correctly the mass remained on walls, and the child droplet diameters for the regime of initial velocities of 2 - 40 m/s and for the region of the initial diameters below 300 micrometers.

The OPT model and the TAB model [2] are combined with the flow code based on the multi-level formulation and the renormalization group theory [3]. The computational results obtained with the code indicate that the secondary atomization behavior on valve-surfaces plays a significant role in the fuel mixture formation in the cylinder of spark-ignition engine.

AN OVAL-PARABOLA TRAJECTORIES (OPT) MODEL OF BREAKUP AFTER DRY-WALL IMPINGEMENT

The breakup process after the impingement of a droplet on a dry wall is modeled. The physical

situation to be modeled is shown in Fig.1.

In Phase A, the parent droplet with the size r_d and the velocity U_p hits the wall and then the droplet is deformed to one with the minimum thickness d_{disc} . The relation between the child droplet size r_2 and the maximum distortion is then derived in Phase B. Then, the number of child droplets n and the size r_1 of the droplet remaining on the wall are estimated in Phase C. Finally, the flying speed of child droplets U_2 is decided.

Determination of child droplet size -

Maximum distortion of parent droplet (Phase A)

$$m \ddot{X} = - C_c \rho_L r_d^2 (\dot{X})^2 - m C_k \frac{\sigma}{\rho_L r_d^3} X - m C_v \frac{\mu}{\rho_L r_d^2} \dot{X} - m C_a \tag{1}$$

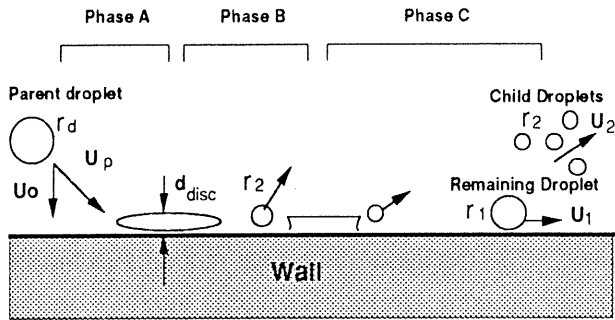


Fig.1 Breakup process after dry-wall impingement

$$\dot{X}_{t=0} = U_0, X_{t=0} = 0 \tag{2}$$

$$m = \frac{4}{3} \pi \rho_L r_d^3 \tag{3}$$

Equation (1) describes the deforming and oscillating motion of a parent droplet from wall-impingement to breakup. First three terms in the right hand side in E. (1) show liquid convection, surface tension, and dissipation contributions. Last term demonstrates the effects by air convection and the heat transfer.

$X, \sigma, \mu, \rho_L, C_c, C_k, C_v$ and C_a demonstrate the representative deformation, surface tension, viscosity coefficient, artificial constants for contributions, respectively.

Equation (2) expresses the initial conditions for the distortion and distortion speed.

In the present report, third and fourth

contributions in the right hadn side of Eq.(1)are eliminated.

These equations are simplified to the following first-order ordinary differential equation system.

$$\dot{X} = Y \tag{4}$$

$$\dot{Y} = - A Y^2 - B X \tag{5}$$

$$A = C_c \frac{\rho_L r_d^2}{m}, B = C_k \frac{\sigma}{\rho_L r_d^3} \tag{6}$$

The trajectory of the system shows a discontinuous transition due to increasing initial velocity [4]. For small initial values of X and Y, the trajectory is an oval in the phase space. For large initial values, the trajectory is a parabola.

When Y equals zero in Fig.2, X gives the value of maximum distortion.

Two finite modes of maximum distortion appear for oval oscillation, while one finite mode and another infinite one appear for parabola.

The deformed droplet shape is assumed to be a disc in the present study. Then the minimum thickness of the disc is determined.

$$X - \frac{1}{2A} [(\frac{2A^2}{B} U_0^2 - 1) \exp(-2AX) + 1] = 0 \tag{7}$$

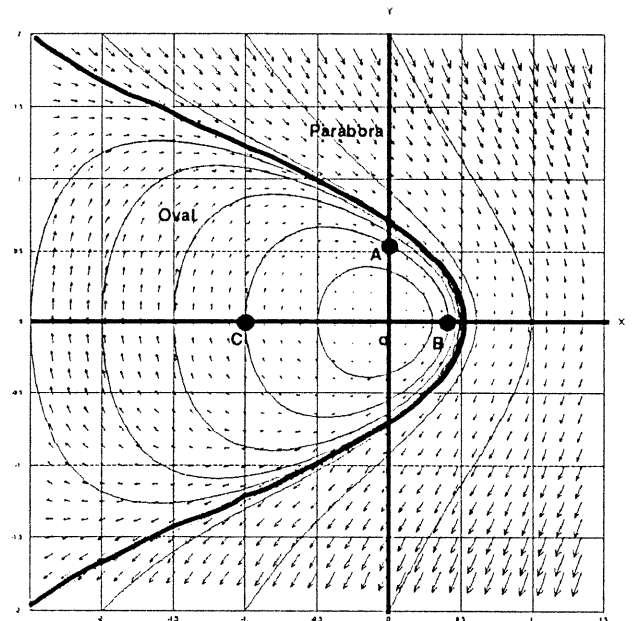


Fig.2 Trajectories in the phase space of the simplified QCODE

Relation between maximum distortion and child droplet size (Phase B) - It is roughly assumed that, when the representative distortion X is over one-half of the initial droplet diameter, the parent droplet breaks up into smaller child droplets and film flow.

Equations (8) and (9) show the mass and energy conservation laws around the edge of deformed droplet at breakup occurrence.

$$V = d_{disc}(\pi r_b^2) = \frac{4}{3} \pi r_2^3 \quad (8)$$

$$E = \pi r_b^2 \sigma = 4\pi r_2^2 \sigma \quad (9)$$

In Eq. (9), the surface energy of the side ring is eliminated. Then

$$r_2 = 3 d_{disc} \quad (10)$$

Equation (10) gives the relation between the size of a child droplet and the thickness of the distorted droplet.

The following four regimes can be proposed as characteristic breakup patterns.

- (1) Permanent coalescence: the maximum distortion is smaller than one-half of the parent droplet size,
- (2) Weak breakup regime with large child droplets of a single size: produced by weak oval oscillation,
- (3) Medium breakup regime with two different droplet size droplets: caused by strong oval oscillation, and
- (4) Strong breakup regime with small droplets: produced by parabolic oscillation.

Determination of the number of child droplets and amount of liquid film remaining on the wall (Phase C)

It is indicated from Eq.(1) that the breakup is possible to occur in two different modes. It is assumed in the present modeling that either one mode among two is selected randomly for each impingement.

Then mass and energy conservation laws between the initial condition before impingement and the situation after breakup are described as follows.

$$\frac{4}{3} \pi \rho_L r_d^3 = n \left(\frac{4}{3} \pi \rho_L r_2^3 \right) + \frac{4}{3} \pi \rho_L r_1^3 \quad (11)$$

$$4\pi r_d^2 \sigma + (1-C_{dis}) \frac{1}{2} \left(\frac{4}{3} \pi \rho_L r_d^3 \right) U_o^2 = n (4\pi r_2^2 \sigma) + 4\pi r_1^2 \sigma \quad (12)$$

Equations (11) and (12) are simplified to the following third-order equation.

$$XX^3 - \frac{r_2}{r_d} XX^2 + \frac{r_2}{r_d} \left[1 + \frac{1}{6\sigma} \rho_L U_o^2 (1-C_{dis}) \right] - 1 = 0 \quad (13)$$

$$XX = \frac{r_1}{r_d} \quad (14)$$

$r_2 = 0$ and $r_1 = r_d$ satisfy the equation under a limited condition of $U_o = 0$ m/s.

Under another limited condition of infinite impingement velocity, Eq.(15) gives the critical droplet size.

$$(r_2)_{crit} = \frac{6\sigma}{1-C_{dis}} \frac{1}{\rho_L U_o^2} \quad (15)$$

Determination of velocity of child droplets- The flight direction of the child droplets is shown in Fig. 3. Equation (16) gives the components of the velocity vector of the child droplets.

$$U_n' = \frac{1}{\sqrt{10}} * \sqrt{rans1} * U_n$$

$$U_{h1}' = \frac{1}{\sqrt{10}} * U_{h1} + \frac{1}{\sqrt{10}} * \sqrt{rans2} * U_n * \cos(2\pi * rans3)$$

$$U_{h2}' = \frac{1}{\sqrt{10}} * \sqrt{rans2} * U_n * \sin(2\pi * rans3) \quad (16)$$

Where rans1, rans2, and rans3 represent the random numbers between zero and one.

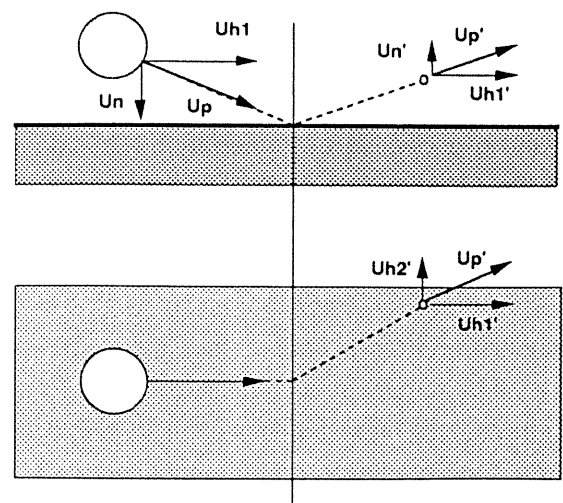


Fig. 3 Flight direction of child droplets

FORMATION OF NUMERICAL CODE FOR FUEL-MIXING PROCESS IN ENGINE

The numerical model for predicting the fuel motions in engines consists of four parts: the subroutine group I for the air flow calculation [3], subroutine group II for spray calculation as that in KIVA II [2] (subroutines for breakup by air-droplet interaction, evaporation-condensation, and drag force), subroutine group III for droplet-wall interaction (the OPT model), and subroutine groups IV for the vapor fuel flow calculation.

FUNDAMENTAL EVALUATIONS OF THE OVAL-PARABOLA TRAJECTORIES (OPT) MODEL

Child droplet size ($U_p=12.0\text{m/s}$, initial diameter $=160\ \mu\text{m}$, Impingement angle = 20, 30, 60 degree) - Droplet impingement at three inclined angles were examined first. Figure 4 shows the histograms of the predicted and measured child droplet sizes, which indicate a bi-modal distribution. This characteristics of bi-modal distribution is explained by the trajectory characteristics of the momentum equation. Another experimental data [7] has also shown the existence of two peaks.

Figure 5 shows the visualization of the breakup processes. The parent droplets do not break into small ones for the impinging angle of 20 degree, both in computation and experiment. The flying directions of child droplets are also predicted well.

Mass remained on wall ($U_o=12, 18, 28, 40\ \text{m/s}$, initial diameter $=100\ \mu\text{m}$) - Next, the mass rate remaining on wall is examined by the comparison with the experimental data [5]. Predictions were obtained only with using the OPT model without flow field calculations. Table 1 shows the mass rates of child droplets for some values of U_o . Both the calculated and the experimental results indicate an increase in percent mass of child droplets produced with increasing impact velocity. The discrepancy between the prediction and the experiment in high-impaction speed regime may be explained by the

fact that predictions in Table 1 doesnot include influence of gravity, evaporation, and turbulene calculations.

	Predicted		Experimental
	Peak D1	Peak D2	
$U_o= 3.50\ (\text{m/s})$	0%	0%	-
12.0 (m/s)	64.5%	26.0%	22%
18.0 (m/s)	81.0%	11.0%	38%
28.0 (m/s)	100.0%	100.0%	48%
40.0 (m/s)	100.0%	100.0%	63%

In the region of U_o of 2 - 40 m/s and the region of initial diameter below 300 , the OPT model predicts several features observed in the experiments including a bimodal distribution of child droplet sizes and an increase in percent mass of child droplets produced with increasing impact velocity.

APPLICATION TO THE FUEL SECONDARY ATOMIZATION PROCESS AND MIXTURE FORMATION IN A SPARK-IGNITION ENGINE

The specifications for the injector and for the engine are listed in Table 2.

Figures 6(a) and (b) demonstrate fuel droplets distributions, calculated with the OPT model and without including the model, respectively. It is understood from Figs. 6(a) and (b) that the air-droplet interaction at the throat of valve is only an assistance for fuel atomization process. The droplet-wall interaction has an decisive role for the formation of fuel vapor cloud in the cylinder. It is also understood that a part of fuel droplets entering into th cylinder impinges to the cylinder wall.

Table 3 shows the mass rate of fuel entering in cylinder. The corresponding experimental data is obtained at an accelerated condition of the engine. The fuel mass taken into the cylinder directly will be 30-40% of the total quantity injected.

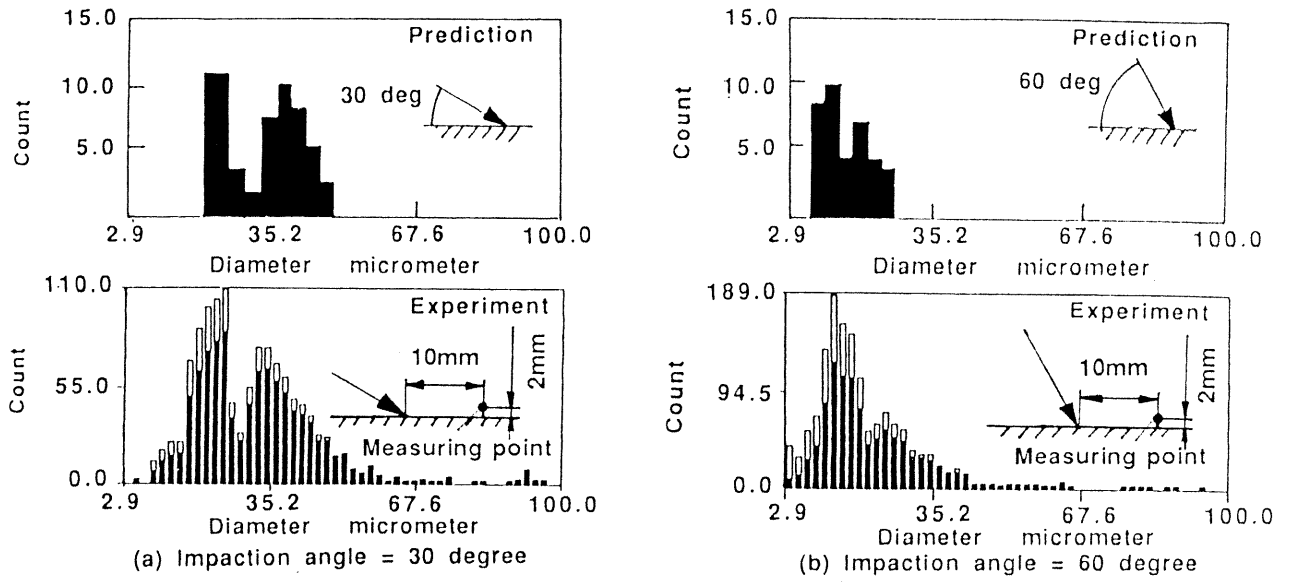


Fig. 4 Distribution of child droplet size

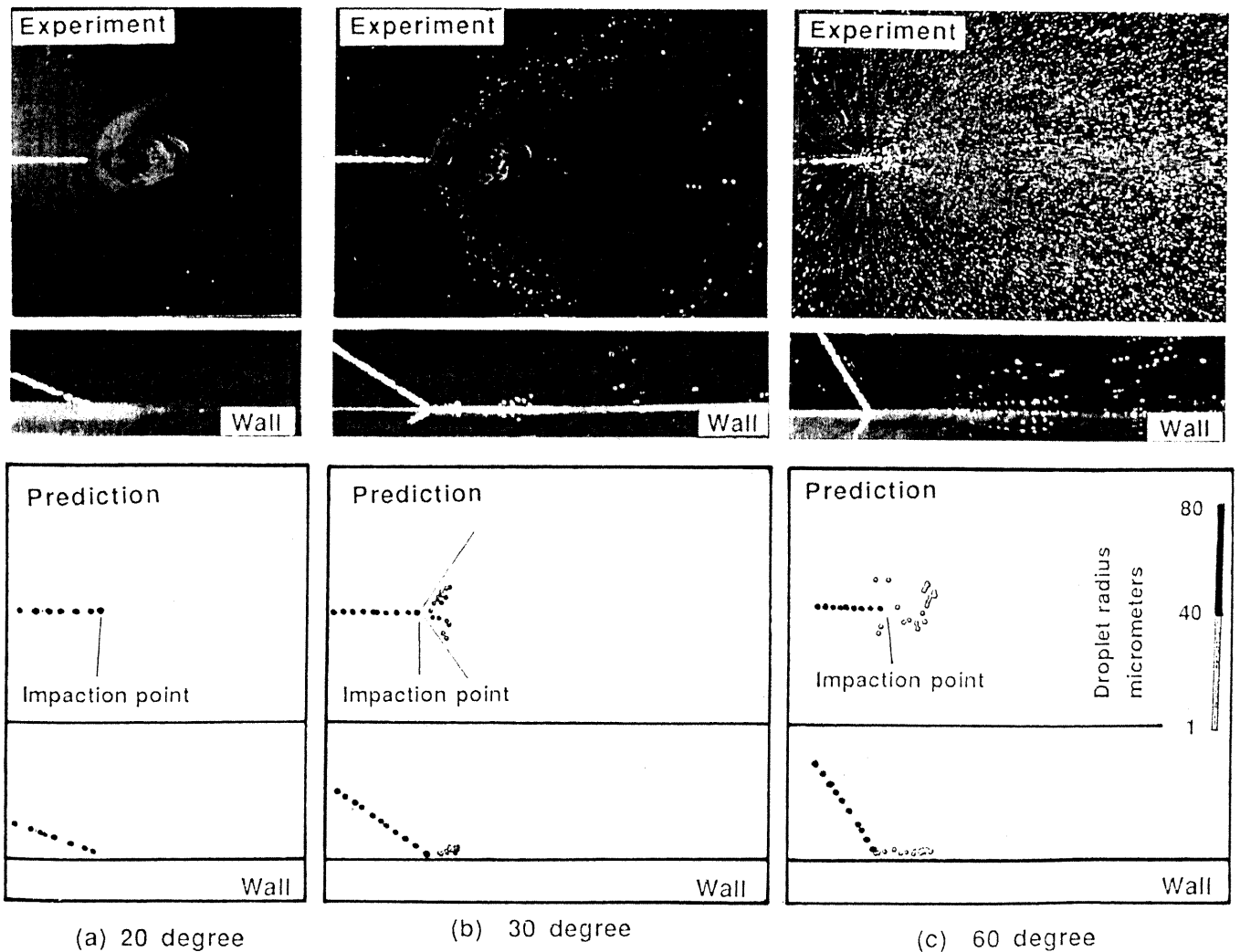


Fig. 5 Visualizations of the breakup process by wall impingement

CONCLUSIONS

A theoretical model for the breakup process after the dry wall impingement of a droplet is developed. It is noteworthy to mention that the model can predict the size of child droplets after wall impingement and the amount of film flow remaining on the wall, for a U_0 range of 2 - 40 m/s and a region of initial diameter below 300 micrometers.

The computational results indicate that the droplet-wall interaction plays an important role for the secondary atomization process in spark-ignition engines.

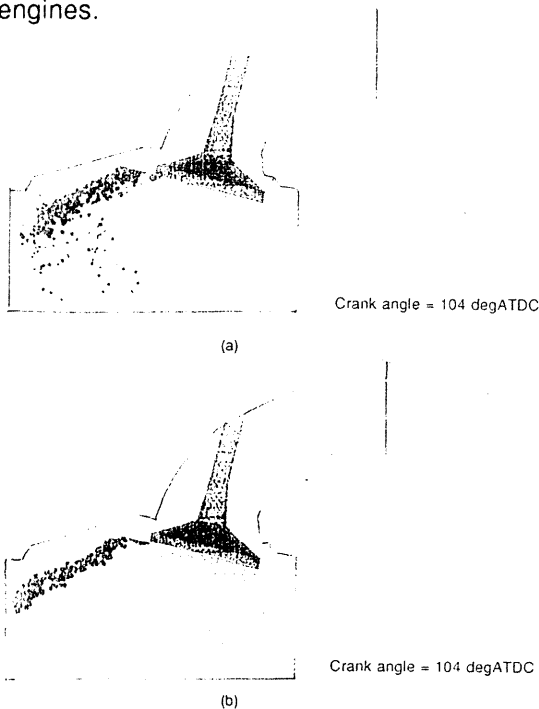


Fig. 6 Fuel droplets motions in the intake ports and cylinder (a) With OPT (b) Without OPT

Table 2 Specifications of injector and engine

Injector (with two spray cones)	
D32	122.0
Cone angle	12.0 degree
Injection velocity	20.0 m/s
Injection timing	0-30 degATDC
Injection angle	29 degree
Engine	
Bore x Stroke	83.0 x 86.0 mm
Engine speed	1200 rpm
A/F ratio	14.8 : 1
Compression ratio	9.0 : 1

Table 3 Amount of fuel entering into cylinder directly

Predicted		Experimental
Without OPT	With OPT	
15%	34.0%	39.0%

ACKNOWLEDGEMENTS

The authors would like to thank Prof. K. Kuwahara of Institute of Space and Astronautical Science and Prof. K. Yamamoto of Waseda University for his much advice on the mathematical aspects.

REFERENCES

1. Reitz, R.D. and Bracco, F.V., "Mechanisms of Atomization of a Liquid Jet", *Phys. Fluids* 25(10), 1982.
2. O'Rourke, P.J. and Amsden, A.A., "The TAB Method for Numerical Calculation of Spray Droplet Breakup", SAEpaper 872089, 1987.
3. Naitoh, K. and Kuwahara, K., "Large Eddy Simulation and Direct Simulation of Compressible Turbulence and Combusting Flows in Engines based on the BI-SCALES method", *J. Fluid Dynamics Research*, 1992.
4. Andronow, A.A. and Chaikin, C.E., "Theory of Oscillations", Princeton University Press, 1949.
5. Suzuki, J., Shimoda, H., and Kodama, H., "Experimental Study on the Atomization of the Array of Droplets Impinging upon the Solid Surface", *Proceedings of the 10th Conference on Liquid Atomization and Spray Systems in Japan*, 1982.
6. Umemura, A., "Collision Behavior of Hydrocarbon Droplets", *Proceedings of Tsukuba International Workshop on Mechanics of Reactive Flows*, 1990.
7. Takeuchi, K., Senda, J., and Sato, Y., *Proceedings of the 9th Japan Conf. on Liquid Atomization and Spray System*, 1981.
8. Naitoh, K., Takagi, Y., Kokita, H., and Kuwahara, K., "Numerical Prediction of Fuel Secondary Atomization Behavior in SI Engine based on the Oval-Parabola Trajectories (OPT) Model", SAEpaper 940526, 1994.